This is the accepted manuscript made available via CHORUS. The article has been published as:

Triplons, triplon pairs, and dynamical symmetries in laser-driven Shastry-Sutherland magnets

Mina Udono and Masahiro Sato

Phys. Rev. B **110**, L201112 — Published 21 November 2024

DOI: 10.1103/PhysRevB.110.L201112

Triplons, triplon pairs and dynamical symmetries in laser-driven Shastry-Sutherland magnets

Mina Udono and Masahiro Sato
Department of Physics, Chiba University, Chiba 263-8522, Japan
(Dated: November 5, 2024)

In frustrated magnets, a variety of novel phenomena arise due to their peculiar magnetic states, whose excitations usually reside in the GHz to THz range. Intense THz lasers, therefore, lead to examining nonlinear optical effects in such magnets. Employing an unbiased numerical method, we calculate the laser-pulse driven harmonic spectra of the Shastry-Sutherland magnets, which are well known as the model of a quantum frustrated magnet $SrCu_2(BO_3)_2$. As a result, nonlinear responses of triplons and a two-triplon bound state are numerically shown to emerge through the Zeeman or magnetoelectric couplings between the laser and the electron spin. Furthermore, the dynamical symmetries and selection rules of harmonic spectra for the Shastry-Sutherland model, realized in $SrCu_2(BO_3)_2$, are derived. The selection rules tell us that one can obtain information on magnetic anisotropy and symmetry from the spectra by manipulating external fields or two-color lasers. Our results indicate that laser-driven harmonic spectra are useful as a probe of less-detectable quantum many-body states in frustrated magnets.

Introduction– Quantum frustrated magnets are a treasure trove of exotic physical phenomena due to the prominent quantum fluctuations and many-body effects. The two-dimensional (2D) spin-$\frac{1}{2}$ Shastry-Sutherland model (SSM) [1], which consists of two types of orthogonal spin dimers, is a typical frustrated magnetic model. The SSM not only shows interesting physical properties due to the peculiar structure but also approximately describes the magnetic properties of $SrCu_2(BO_3)_2$ (SCBO) [2–12], which Kageyama synthesized in 1999 [13]. Various phenomena have been discovered in SCBO [14–26].

The SSM possesses an intradimer interaction $J(>0)$ and interdimer one $J'(>0)$, and its lattice and unit cell are shown in Fig. 1(a) and (b), respectively. The ground state of the SSM has at least two phases depending on the ratio of J to J': One is a dimer singlet phase (DSP) with a spin gap in the $J \gg J'$ limit and the other is a gapless antiferromagnetic (i.e., Néel) ordered state in the $J \ll J'$ limit. The intermediate phase between these two phases is considered to be the plaquette state with four spins forming a singlet [27–29]. The ground-state phase diagram of the SSM is depicted in Fig. 1(c) [27, 30, 31]. The SCBO with $J'/J \simeq 0.635$, whose ground state is in the DSP [13, 32], is close to the quantum critical point of $J'/J \simeq 0.67$ between the dimer singlet and plaquette phases. A plaquette phase has indeed been realized by applying a huge pressure to SCBO [33–39] and its properties have been actively explored. In addition to pressure, an external magnetic field is generally useful to generate novel phases in frustrated magnets. In fact, several magnetization plateau phases have been observed and investigated in SCBO [13, 40–52].

Many experimental techniques are available to observe exotic properties of frustrated magnets including SCBO. For instance, measurements of magnetization, susceptibilities, and specific heat are very powerful to see static properties. Nuclear magnetic resonance, electron spin resonance, neutron scattering, thermal transport and Raman scattering are useful to investigate dynamical natures or excitations in magnets.

Besides these established methods, THz-laser techniques (electromagnetic waves in 10^{11-13} Hz range) have been developed in the last decades [53–61]. THz-photon energies (0.1-10 meV) are comparable to those of magnetic excitations. Hence, THz waves are very useful to directly observe such excitations [58, 62–76]. In fact, various magnetic quasiparticles like magnons [58, 63–72], electromagnons [73–75], magnetic solitons [76], etc. have been detected with THz-wave methods. Moreover, quite recently, the harmonic generation (HG) up to the third harmonic via magnetic excitations (without any photo-induced electron transition) has been observed by applying intense THz pulses to an antiferromagnet [77]. In addition to experiments, THz-wave induced phenomena have been theoretically predicted: Control of magnetic states with intense THz wave [78], THz-laser-driven nonlinear responses in quantum spin chains [79, 80], spin-nematic magnets [81], and Kitaev magnets [82], and Floquet engineering of magnets [83–89].

In this paper, motivated by these activities, we theoretically explore the THz-laser-driven nonlinear optical response of the SSM with/without some perturbations. From the theoretical viewpoint, numerical studies of non-equilibrium many-body states in 2D models are challenging because it is generally difficult to analyze sufficiently large 2D systems due to computational cost. However, by using an unbiased numerical method for finite-size systems, we obtain reliable results about the THz-pulse-induced spin dynamics in the SSMs. We mainly focus on the DSP realized in SCBO, where triplons with spin $S = 1$ and two-triplon bound states (triplon pairs) appear as the low-energy excitations [4, 8, 17, 20, 44, 90–93]. We show that triplons or a triplon pair are excited by a THz pulse, and first- to third-order harmonics are ob-

served depending on the sorts of light-matter couplings (Zeeman and magnetoelectric couplings) and the light polarization direction. Namely, the dynamical symmetries [79, 82, 94–98] associated with the light-matter coupling are shown to drastically change the selection rule (appearance or absence) of the n-th order harmonics. We find that the selection rule quite differs from those in photo-driven electron systems accompanying electric dipole transition, and it can be controlled by introducing static perturbations (like external magnetic fields) or deforming the laser shape from single- to two-color type. Our result indicates that THz-laser response can be a powerful tool to detect less-detectable natures of many-spin states in a broad class of magnets.

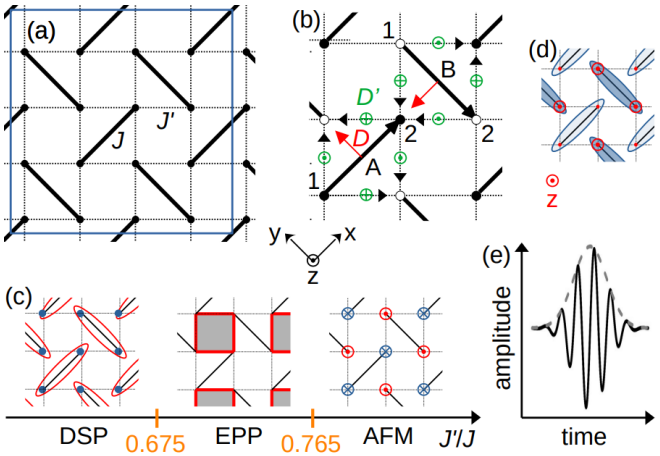


FIG. 1. (a) Lattice of SSM. Thick and thin dashed lines, respectively, indicate the intradimer and interdimer antiferromagnetic interactions. Our calculation employs the 16-site square cluster, surrounded by the blue line. (b) Symmetry allowed intradimer (red) and interdimer (green) DM vectors in a unit cell. Each black arrow from i to j shows the ordering of two spin operators $\hat{\boldsymbol{S}}_i \times \hat{\boldsymbol{S}}_j$ in the DM term on the i-j bond. Orthogonal dimers (thick continuous lines) are denoted by A (consists of filled circle sites) and B (consists of open circle sites); spin sites on the dimer are numbered 1 and 2. The $\hat{S}^\alpha$ axis is parallel to the real-space α axis depicted below the panel (b). (c) Ground-state phase diagram of the SSM. The DSP, EPP, and AFM refer to the dimer singlet phase, the empty plaquette phase, and the antiferromagnetic phase, respectively [30]. (d) Spin configuration of the 1/2 magnetization plateau phase (PP). Two distinct dimers exist; dimers with $\langle \hat{S}^z_j \rangle = 1/4 + \delta$ (red double circles) and ones with $\langle \hat{S}^z_j \rangle = 1/4 - \delta$ (small red circles). (e) Schematic of Gaussian pulse used in our simulations. The dashed line indicates the Gaussian envelope.

Model and Methods– The target of this study is the Shastry-Sutherland model (SSM), whose Hamiltonian is

$$\hat{\mathscr{H}}_{\rm SS} = J' \sum_{\langle {\rm i.j} \rangle} \hat{\boldsymbol{S}}_i \cdot \hat{\boldsymbol{S}}_j + J \sum_{\langle\langle {\rm i.j} \rangle\rangle} \hat{\boldsymbol{S}}_i \cdot \hat{\boldsymbol{S}}_j, \qquad (1)$$

where $\hat{\boldsymbol{S}}_j$ is the spin-$\frac{1}{2}$ operator on j-th site. As shown in Fig. 1(a), J and J' are the intradimer and interdimer interactions, respectively. We set J as a unit of energy and choose $J'/J = 0.5$, where the ground state is the DSP that we mainly focus on. Under a DC magnetic field, the Zeeman term $\hat{\mathscr{H}}_{\rm Zeeman} = -\sum_i \boldsymbol{h} \cdot \hat{\boldsymbol{S}}_i$ is added. Here, $h_\alpha = g_\alpha \mu_{\rm B} H^\alpha$, $(\alpha = x,\ z)$, where g_α is the g-tensor, $\mu_{\rm B}$ is the Bohr magneton, and H^α is the magnetic field.

In addition to the exchange interactions, the crystal structure of SCBO allows the emergence of Dzyaloshinskii-Moriya (DM) interactions [99, 100]

$$\hat{\mathscr{H}}_{\rm DM} = \sum_{\langle {\rm i.j} \rangle} \boldsymbol{D}'_{ij} \cdot (\hat{\boldsymbol{S}}_i \times \hat{\boldsymbol{S}}_j) + \sum_{\langle\langle {\rm i.j} \rangle\rangle} \boldsymbol{D}_{ij} \cdot (\hat{\boldsymbol{S}}_i \times \hat{\boldsymbol{S}}_j), \quad (2)$$

where $\boldsymbol{D}'_{ij}$ and $\boldsymbol{D}_{ij}$ are the interdimer and intradimer DM vectors, respectively. Figure 1(b) shows the ordering of i- and j-site spins in each DM term $\hat{\boldsymbol{S}}_i \times \hat{\boldsymbol{S}}_j$; $\boldsymbol{D}'_{ij} = (0, 0, D')$ for interdimer bonds, and $\boldsymbol{D}_{ij} = (0, D, 0)$ $[(-D, 0, 0)]$ for A [B] intradimer bonds [2, 5, 8, 14, 23, 46, 101–105]. For SCBO, the interdimer DM terms explain the splitting observed in the lowest branch of the triplon excitation in zero field [5], while the intradimer DM terms mix the ground singlet state with the triplon, which explains the anti-crossing observed in the experiment [20, 106]. When only D' is finite, the system possesses U(1) symmetry, but the introducing D destroys this symmetry. SCBO exhibits a structural transition at 395 K [8, 107], below which the symmetry is lowered. The DM term with D' (D) is relevant to the high and low temperature phases (low temperature phase) of SCBO. We examine the U(1) breaking case, and the parameters are chosen to be $D' = 0.015J$ and $D = 0.025J$ except for Fig. 4 dealing with the SU(2) symmetric case.

Next, we consider the light-matter coupling. The fundamental coupling in spin systems is the AC Zeeman interaction whose Hamiltonian is $\hat{\mathscr{H}}_{\rm Zeeman}(t) = -\sum_i \boldsymbol{h}_{\rm p}(t) \cdot \hat{\boldsymbol{S}}_i$, where $h^\alpha_{\rm p}(t) = g_\alpha \mu_{\rm B} H^\alpha_{\rm p}(t)$ and $\boldsymbol{H}_{\rm p}(t)$ is the laser magnetic field. In addition to it, multiferroic magnets including SCBO can be coupled to the electric field of the laser through magnetoelectric (ME) coupling [73, 74, 108–115], which means the interaction between electric polarization $\hat{\boldsymbol{P}}$ and electron spin. The polarization $\hat{\boldsymbol{P}}$ interacts with the applied laser via the Hamiltonian $\hat{\mathscr{H}}_{\rm ME}(t) = -\boldsymbol{E}_{\rm p}(t) \cdot \hat{\boldsymbol{P}}$, where $\boldsymbol{E}_{\rm p}(t)$ is the electric field of laser. As a result, spins in multiferroics are coupled to the electric field of the laser as well. According to Ref. [106, 115–117], SCBO has two types of ME couplings: The first is the exchange-striction type [73, 112] of ME coupling on the J' bond, whose Hamiltonian is given by

$$\hat{\boldsymbol{P}}_{\rm S} = \sum_{\langle {\rm i.j} \rangle} \Pi_{\rm me} \boldsymbol{e}_{ij} \hat{\boldsymbol{S}}_i \cdot \hat{\boldsymbol{S}}_j, \qquad (3)$$

where $\Pi_{\rm me}$ is the coupling constant and $\boldsymbol{e}_{ij}$ is the unit vector pointing from i to j sites on a J' bond. The second

ME interaction is the so-called inverse DM type [74, 109, 112, 118, 119] on the J bond and the Hamiltonian [115] is

$$\hat{\boldsymbol{P}}_{\rm AS} = \sum_{\langle\langle {\rm i,j}\rangle\rangle} D_{\rm me}\boldsymbol{e}_{ij} \times \left(\hat{\boldsymbol{S}}_i \times \hat{\boldsymbol{S}}_j\right), \tag{4}$$

where $D_{\rm me}$ is the coupling constant and $\boldsymbol{e}_{ij}$ is defined on a J bond. For the laser fields $\boldsymbol{E}_{\rm p}(t)$ and $\boldsymbol{H}_{\rm p}(t)$, we adopt a Gaussian pulse $\boldsymbol{A}(t) = \boldsymbol{A}\sin(\omega_{\rm p}(t-t_0))\exp\left(-(t-t_0)^2/2\sigma_{\rm p}^2\right)$, as shown in Fig. 1(e), with the frequency $\omega_{\rm p}$ and the pulse width $\sigma_{\rm p}$ centered at time t_0. Here, $\boldsymbol{A}(t) = \boldsymbol{E}_{\rm p}(t)$ or $\boldsymbol{H}_{\rm p}(t)$, and $\boldsymbol{A}$ denote the amplitudes $\boldsymbol{E}_{\rm p}$ or $\boldsymbol{H}_{\rm p}$. Unless otherwise noted, when we consider the dynamics of the α component of electric polarization $\hat{P}^\alpha$ (magnetization $\hat{M}^\alpha = \sum_i g_\alpha \mu_{\rm B}\hat{S}_i^\alpha$), we apply an AC electric field $E_{\rm p}^\alpha(t)$ (magnetic field $H_{\rm p}^\alpha(t)$) with the same polarization direction to the SSM.

The light-spin coupling is generally much smaller than the light-charge one, and it is difficult to detect the nonlinear optical responses in spin systems. However, as we already mentioned, we can apply sufficiently intense THz laser to materials with currently available techniques [53–61]. In multiferroics, the ME-coupling strengths of $\Pi_{\rm me}$ and $D_{\rm me}$ depend on the detail of materials and frequency, and they can be comparable to that of Zeeman interaction in materials with a strong enough ME coupling, i.e., $|\Pi_{\rm me}E_{\rm p}| \sim |D_{\rm me}E_{\rm p}| \sim |g_\alpha\mu_{\rm B}H_{\rm p}^\alpha|$. Hereafter, we suppose that the SSM has such a strong ME coupling. In fact, recent experiments show that SCBO has a large ME coupling of Eq. (3) [106, 120].

We note again that THz- and GHz-photons' energies are usually much smaller than the charge excitation gap of Mott insulators including SCBO, making the light-charge coupling irrelevant. In fact, THz-laser-driven magnetic modes without charge excitations have been detected in many experiments [58, 62–77]. Therefore, it is sufficient to consider only light-spin couplings without light-charge ones when we apply THz or GHz waves to the SSM.

We calculate expectation values of the electric polarization $\hat{\boldsymbol{P}}$ and the magnetization $\hat{\boldsymbol{M}}$ as a function of time, using the numerical Lanczos method [121–123] in the 16-site cluster, which is invariant under the operations for $\pi/2$ rotation of lattice [124]. The simulation is done in a finite time range $[0, t_{\rm max}]$, and the dissipation effect is not included in the ED method. Therefore, we should introduce a window function $w(t) = 0.54 - 0.46\cos(2\pi t/(t_{\rm max}-1))$ to obtain realistic harmonics spectra via an effective Fourier transformation [125, 126]. Namely, for the expectation value of a physical quantity $O(t)$, we define its spectrum as $O(\omega) = \int_0^{t_{\rm max}} O(t)w(t)e^{i\omega t}{\rm d}t$. We will use symbols $P_{\rm S}^\alpha(\omega)$, $P_{\rm AS}^\alpha(\omega)$ and $M^\alpha(\omega)$ as the effective Fourier transforms of $\langle\hat{P}_{\rm S}^\alpha(t)\rangle$, $\langle\hat{P}_{\rm AS}^\alpha(t)\rangle$, and $\langle\hat{M}^\alpha(t)\rangle$, respectively. In the simulations, the strengths of light-matter couplings are fixed to $|\Pi_{\rm em}E_{\rm p}| = 0.1J$, $|D_{\rm em}E_{\rm p}| = 0.1J$ or $|g_\alpha\mu_{\rm B}H_{\rm p}^\alpha| = 0.2J$ unless otherwise noted. One can approach these large values by using a THz pulse with a strong electric field of ~ 1MV/cm.

Results– Below we show several important findings of our numerical computation, features of THz-pulse driven dynamics in the SSM. More details are in Supplemental Material (SM) [127].

A: Electric polarizations– In the main text, we concentrate on the dynamics driven by ME couplings. That driven by AC Zeeman coupling is in the SM [127]. The main mode excited by $\hat{\boldsymbol{P}}_{\rm S}$ is the triplon bound state with $S = 0$ (resonance frequency $\omega/J \sim 1.2$), while that by $\hat{\boldsymbol{P}}_{\rm AS}$ is the single triplon (resonance frequency $\omega/J \sim 0.7$) [4, 115]. Figure 2 shows the harmonic spectra $P_{\rm S}^\alpha(\omega)$ ($\alpha = x,\ y$) driven by a light-matter coupling $\hat{\mathscr{H}}_{\rm ME}(t) = -E_{\rm p}^\alpha(t)\hat{P}_{\rm S}^\alpha$ and $P_{\rm AS}^\alpha(\omega)$ ($\alpha = x,\ y,\ z$) by $-E_{\rm p}^\alpha(t)\hat{P}_{\rm AS}^\alpha$ in the model with $\boldsymbol{H} = \boldsymbol{0}$. The laser frequency $\omega_{\rm p}$ is chosen to their resonance frequencies. Besides the fundamental harmonic, third-order one is also observed, but even-order responses do not appear. The fundamental (linear) responses of $P_{\rm S}^\alpha(\omega_{\rm p})$ and $P_{\rm AS}^\alpha(\omega_{\rm p})$ are consistent with those of a numerical study for a larger system [115], which means that our results for 16-site clusters can capture the thermodynamic nature in a semi-quantitative level. Figure 2 also indicates that nonlinear third harmonics can be observed by utilizing currently available intense THz laser. When a static magnetic field is applied, we verify that the spectral peak of $\hat{\boldsymbol{P}}_{\rm AS}$ exhibits the Zeeman splitting, while that of $\hat{\boldsymbol{P}}_{\rm S}$ does not. This is a clear evidence for detecting triplons and triplon pairs in Fig. 2. The splitting is explained in more detail in Supplemental Material (SM) [127]. Here we remark two things: The first is that tirplons and triplon pairs with only a certain wave vector (typically $\boldsymbol{k} = \boldsymbol{0}$) are detected by the HG because applied waves have a long wavelength and may be viewed as a spatially uniform field for electron spins. Secondly, small spikes in the HG spectra are expected to be negligible in the real materials (for more detail, see SM).

B: Dynamical symmetries in DSP– Next, we consider the selection rule of the n-th order harmonics of the SSM. To this end, it is important to find a dynamical symmetry of the periodically driven system, in which the laser pulse should be replaced with an ideal continuous wave ($\sigma_{\rm p} \to \infty$). If a time-periodic system with a Hamiltonian $\hat{\mathscr{H}}(t) = \hat{\mathscr{H}}(t+T_{\rm p})$ ($T_{\rm p}$ is the time period) satisfies the relation $\hat{U}\hat{\mathscr{H}}(t+T_{\rm p}/m)\hat{U}^\dagger = \hat{\mathscr{H}}(t)$ with $m \in \{2,3,\cdots\}$ and $\hat{U}$ being a symmetry operator, one says that the system possesses the dynamical symmetry associated with the symmetry of $\hat{U}$. In laser-driven systems, $T_{\rm p} = 2\pi/\omega_{\rm p}$ stands for the period of the laser. One can often find a selection rule of harmonic spectra in dynamically symmetric systems. For more details of the dynamical sym-

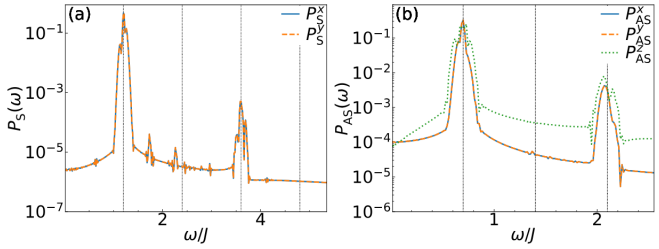


FIG. 2. Computed HG spectra of (a) $\boldsymbol{P}_{\rm S}(\omega)$ and (b) $\boldsymbol{P}_{\rm AS}(\omega)$ under zero field $\boldsymbol{H}=\boldsymbol{0}$. Blue and orange lines in both figures represent the x and y components of the electric polarizations, respectively, while the green line in (b) shows the z component of $\boldsymbol{P}_{\rm AS}(\omega)$. Vertical dotted lines represent integer multiples of $\omega_{\rm p}$. For $J=1$ meV, $\omega=J$ corresponds to 2.42×10^{11} Hz.

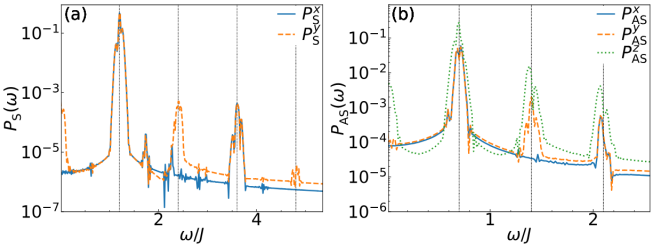


FIG. 3. HG spectra of (a) $\boldsymbol{P}_{\rm S}(\omega)$ and (b) $\boldsymbol{P}_{\rm AS}(\omega)$ calculated with $h_x/J=0.1$. Blue and orange lines in all figures represent the x and y components of $\boldsymbol{P}_{\rm S}(\omega)$ or $\boldsymbol{P}_{\rm AS}(\omega)$, respectively, while the green line in (b) shows the z component of $\boldsymbol{P}_{\rm AS}(\omega)$. Vertical dotted lines represent integer multiples of $\omega_{\rm p}$.

metry, see SM [127]. We can find dynamical symmetries of $\hat{U}\hat{\mathscr{H}}(t)\hat{U}^{-1}=\hat{\mathscr{H}}(t+T_{\rm p}/2)$ when the total Hamiltonian is given by $\hat{\mathscr{H}}(t)=\hat{\mathscr{H}}_{\rm SS}+\hat{\mathscr{H}}_{\rm DM}+\hat{\mathscr{H}}_{\rm ME}(t)$, and the symmetry operator $\hat{U}$ is chosen to be $C_2(z)$ or σ_{yz} for $E^x_{\rm p}$, $C_2(z)$ or σ_{zx} for $E^y_{\rm p}$, and S_4 for $E^z_{\rm p}$ [8, 128, 129]. However, except for σ_{yz} (σ_{zx}), they are broken when a DC magnetic field $h_{x(y)}$ (together with an intradimer DM interaction) is introduced. The spectra $\boldsymbol{P}_{\rm S(AS)}(\omega)$ with the DC magnetic field h_x are shown in Fig. 3. Figure 2 shows that in the cases of $h_x=0$, there is no dynamical symmetry breaking and any even-order peak disappears, whereas Fig. 3 shows that under a magnetic field $h_x\neq0$, the dynamical symmetry about $P^y_{\rm S}(\omega)$ and $P^{y,z}_{\rm AS}(\omega)$ are broken (that of $P^x_{\rm S(AS)}(\omega)$ survives) and the even-order responses for these polarizations are observed. The selection rule for even-order harmonics in electron systems is always governed by an inversion symmetry, while we emphasize that in the case of magnetic-excitation induced harmonics [77, 79, 82, 96, 97], several selection rules associated with different symmetries can appear depending on the spin-light couplings and static symmetries of the systems. The above selection rule also indicates that an external magnetic field and its direction can control the breaking of dynamical symmetries. More details of selection rules are summarized in SM.

C: Two-color laser– In the above paragraphs, we show that the harmonic spectra can be controlled by a static term in the Hamiltonian like a DC magnetic field and a DM interaction. However, dynamical symmetries can also be dependent on the shape of the laser field. Here, we consider the possibility of controlling the spectra by changing the laser wave shape. For this purpose, we deal with a bicircular laser, a combination of a left circularly polarized light (CPL) with frequency $\omega_{\rm p}$ and a right CPL with $\ell\omega_{\rm p}$. The electric field $\boldsymbol{E}_{\rm p}(t)$ of the bicircular laser is given by

$$\begin{aligned}\boldsymbol{E}_{\rm p}(t)&=\boldsymbol{E}_{\rm p}e^{-(t-t_0)^2/2\sigma_{\rm p}^2}\left(\boldsymbol{E}_{\rm p1}(t)+\boldsymbol{E}_{\rm p2}(t)\right)/\sqrt{2},\\ \boldsymbol{E}_{\rm p1}(t)&=\left[\cos(\omega_{\rm p}(t-t_0))\hat{\boldsymbol{e}}^x+\sin(\omega_{\rm p}(t-t_0))\hat{\boldsymbol{e}}^y\right],\\ \boldsymbol{E}_{\rm p2}(t)&=\left[\cos(\ell\omega_{\rm p}(t-t_0))\hat{\boldsymbol{e}}^x-\sin(\ell\omega_{\rm p}(t-t_0))\hat{\boldsymbol{e}}^y\right],\end{aligned}\quad(5)$$

where the $\boldsymbol{E}_{\rm p1}(t)$ [$\boldsymbol{E}_{\rm p2}(t)$] is the field of the left [right] CPL, and $\hat{\boldsymbol{e}}^x$ ($\hat{\boldsymbol{e}}^y$) is the unit vector of x (y) direction. The integer ℓ represents the multiple of the laser frequency with respect to the first laser. Figure 4 (a) depicts the trajectory of the bicircular laser with $\ell=2$ and it leads to a different spacial symmetry from linearly or circularly polarized light. These sorts of multiple-color lasers are applicable with the current laser techniques [130–134]. Figure 4 (b) shows the spectra $P^{x,y}_{\rm S}(\omega)$ under this bicircular light with $\ell=2$ in the SU(2)-symmetric SSM with $D=0$, $D'=0$ and $\boldsymbol{H}=\boldsymbol{0}$. The SSM does not have the three-fold rotational symmetry, in other words, incompatible with the symmetry of the bicircular light. It means that no symmetry operator $\hat{U}$ satisfies the dynamical symmetry $\hat{U}\hat{\mathscr{H}}(t)\hat{U}^{-1}=\hat{\mathscr{H}}(t+T_{\rm p}/\ell)$ for $\ell=2$ even though the total Hamiltonian keeps the SU(2) symmetry without DM interactions. As a result, all the integer order responses, including the peaks with multiples of 3, appear as shown in Fig. 4(b). Choosing the two lasers to have a four-fold rotational symmetry shown in Figure 4 (c), dynamical symmetry is not broken, and even-order does not appear. We deal with its detail in the SM [127].

D: Ordered phases– So far, we have focused on the THz-laser-driven dynamics in the DSP, which is relevant to SCBO. As we mentioned in the Introduction, if we introduce a strong enough perturbation like a pressure or a magnetic field, SCBO enters other phases accompanying a spontaneous symmetry breaking. Here, we analyze the harmonic spectra in the $\frac{1}{2}$ plateau phase (PP) [see Fig. 1 (d)]. In the PP, two sorts of dimers respectively have different values of magnetizations, and as a result, the S_4 symmetry is spontaneously broken [127]. To realize this phase in our finite 16-site cluster, we ap-

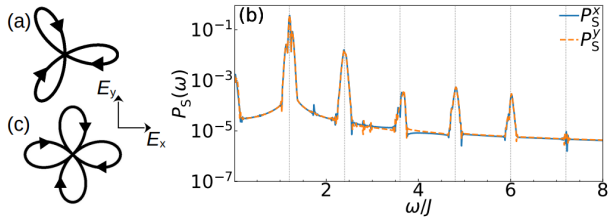


FIG. 4. (a) Trajectory of the laser field of bicircular light [Eq. (5) in $l = 2$] with 3-fold rotational symmetry. (b) Harmonic spectra $\boldsymbol{P}_{\rm S}(\omega)$ under the bicircular light in the SU(2) model with $D = 0$, $D' = 0$, and $\boldsymbol{H} = \boldsymbol{0}$. Blue and orange lines respectively represent $P^x_{\rm S}(\omega)$ and $P^y_{\rm S}(\omega)$. Vertical dotted lines represent integer multiples of $\omega_{\rm p}$. (c) Trajectory of the laser field of bicircular light [Eq. (5) in $l = 3$] with 4-fold rotational symmetry.

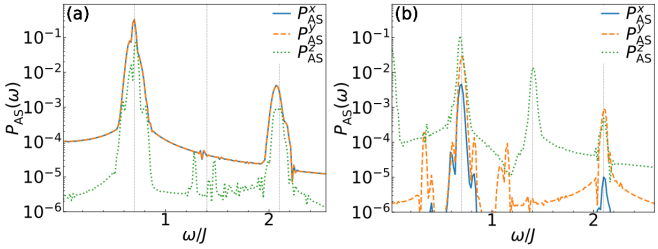


FIG. 5. $\boldsymbol{P}_{\rm AS}(\omega)$ (a) in the DSP with $h_z/J = 0.1$ and $h_{\rm s} = 0$ and (b) in the $\frac{1}{2}$ PP with $h_z/J = 1.5$ and $h_{\rm s}/J = 0.01$. Even-order harmonic peaks of $P^z_{\rm AS}$, which does not exist in the DSP, appear in the PP. Blue, orange, and green lines in both figures represent the x, y, and z components of $\boldsymbol{P}_{\rm AS}(\omega)$. Vertical dotted lines represent integer multiples of $\omega_{\rm p}$.

ply a small alternating magnetic field to bonds A and B as the mean field [135]: Namely, we add a perturbation $\hat{\mathscr{H}}_{\rm bias} = -h_{\rm s}\left(\sum_{i\in{\rm A}}\hat{S}^z_i - \sum_{i\in{\rm B}}\hat{S}^z_i\right)$, which is equivalent to the order parameter in this phase. Recalling that the dynamical symmetry with $\hat{U} = S_4$ is relevant to $E^z_{\rm p}$, it is expected that $P^z_{\rm AS}(\omega)$ shows even-order responses in the PP with light-matter coupling $\hat{\mathscr{H}}_{\rm ME}(t) = -E^z_{\rm p}(t)P^z_{\rm AS}(\omega)$. The estimated electric polarizations $P^\alpha_{\rm AS}(\omega)$ in the DSP and PP are depicted in Fig. 5 (a) and (b), respectively. We numerically verify that for $J'/J = 0.5$, the $\frac{1}{2}$ PP exists in the range $1.1 \lesssim h_z/J \lesssim 1.9$, and therefore we set $h_z/J = 1.5$ to estimate the harmonic spectrum in the PP. Figure 5 shows that in the PP, even-order harmonics of $P^z_{\rm AS}(\omega)$ appear, whereas there is no even-order peak in the DPS. This result indicates that the selection rule for harmonic spectra changes by ordering patterns. It means that we can detect important information about magnetic order and symmetry breakdowns by observing THz-laser-driven harmonic spectra. Similar breakings of dynamical symmetries can occur in other ordered phases such as plaquette ordered phases [Fig. 1 (c)] and spin-nematic phase predicted in Ref. [136]. These dynamical symmetry breakdowns and the change of the selection rules due to the emergence of orders will be explained in SM [127].

Summary– In summary, we have numerically investigated the THz-laser-driven nonlinear responses of the SSM with/without the DM interactions, which could be observed in SCBO. Triplons are detectable in the electric polarization $\boldsymbol{P}_{\rm AS}(\omega)$, while triplon pairs are in $\boldsymbol{P}_{\rm S}(\omega)$. We demonstrate that the selection rule of the HG spectra in the SSM can be controlled by manipulating a DC magnetic field, DM interactions, and the shape of laser. Moreover, we find that the rule is also changed depending on the ordering patterns in the SSM.

In magnets, the SU(2) spin-rotational and spatial symmetries are often broken in various manners, depending on magnetic orders and anisotropies. Our results indicate that THz or GHz wave driven HG spectra are powerful in obtaining the important properties of quasiparticles, magnetic orderings, and the sorts of light-matter couplings in broad phases of magnets. This is in contrast with semiconductors and metals, in which the HG spectra are usually used to detect only the inversion symmetry breaking.

The authors would like to thank Shunsuke Furukawa for his valuable comments and support for the numerical method. This work was supported by KAKENHI (Grant No. JP20H01849), a Grant-in-Aid for Scientific Research on Innovative Areas "Evolution of Chiral Materials Science using Helical Light Fields" (Grants No. JP22H05131 and No. JP23H04576) from JSPS of Japan, and JST, CREST Grant Number JPMJCR24R5, Japan. M.U. acknowledges the support by JST SPRING (Grant No. JPMJSP2109). The numerical diagonalization program is based on the package TITPACK ver.2.

[1] B. Sriram Shastry and B. Sutherland, Exact ground state of a quantum mechanical antiferromagnet, Physica B+C **108**, 1069 (1981).
[2] S. Miyahara and K. Ueda, Theory of the orthogonal dimer heisenberg spin model for $SrCu_2(BO_3)_2$, Journal of Physics: Condensed Matter **15**, R327 (2003).
[3] C. Knetter, A. Bühler, E. Müller-Hartmann, and G. S. Uhrig, Dispersion and symmetry of bound states in the shastry-sutherland model, Phys. Rev. Lett. **85**, 3958 (2000).
[4] K. Totsuka, S. Miyahara, and K. Ueda, Low-lying magnetic excitation of the shastry-sutherland model, Phys. Rev. Lett. **86**, 520 (2001).
[5] O. Cépas, K. Kakurai, L. P. Regnault, T. Ziman, J. P. Boucher, N. Aso, M. Nishi, H. Kageyama, and Y. Ueda, Dzyaloshinski-moriya interaction in the 2d spin gap system $SrCu_2(BO_3)_2$, Phys. Rev. Lett. **87**, 167205 (2001).
[6] H. Kageyama, Y. Ueda, Y. Narumi, K. Kindo, M. Kosaka, and Y. Uwatoko, Crossbreeding between experiment and theory on orthogonal dimer spin sys-

tem, Progress of Theoretical Physics Supplement **145**, 17 (2002).
[7] C. Knetter and G. S. Uhrig, Dynamic structure factor of the two-dimensional shastry-sutherland model, Phys. Rev. Lett. **92**, 027204 (2004).
[8] J. Romhányi, K. Totsuka, and K. Penc, Effect of dzyaloshinskii-moriya interactions on the phase diagram and magnetic excitations of $SrCu_2(BO_3)_2$, Phys. Rev. B **83**, 024413 (2011).
[9] P. Corboz and F. Mila, Crystals of bound states in the magnetization plateaus of the shastry-sutherland model, Phys. Rev. Lett. **112**, 147203 (2014).
[10] A. Wietek, P. Corboz, S. Wessel, B. Normand, F. Mila, and A. Honecker, Thermodynamic properties of the shastry-sutherland model throughout the dimer-product phase, Phys. Rev. Res. **1**, 033038 (2019).
[11] J. L. Jiménez, S. P. G. Crone, E. Fogh, M. E. Zayed, R. Lortz, E. Pomjakushina, K. Conder, A. M. Läuchli, L. Weber, S. Wessel, A. Honecker, B. Normand, C. Rüegg, P. Corboz, H. M. Rønnow, and F. Mila, A quantum magnetic analogue to the critical point of water, Nature **592**, 370 (2021).
[12] Z. Shi, S. Dissanayake, P. Corboz, W. Steinhardt, D. Graf, D. M. Silevitch, H. A. Dabkowska, T. F. Rosenbaum, F. Mila, and S. Haravifard, Discovery of quantum phases in the shastry-sutherland compound $SrCu_2(BO_3)_2$ under extreme conditions of field and pressure, Nature Communications **13**, 2301 (2022).
[13] H. Kageyama, K. Yoshimura, R. Stern, N. V. Mushnikov, K. Onizuka, M. Kato, K. Kosuge, C. P. Slichter, T. Goto, and Y. Ueda, Exact dimer ground state and quantized magnetization plateaus in the two-dimensional spin system $SrCu_2(BO_3)_2$, Phys. Rev. Lett. **82**, 3168 (1999).
[14] M. Takigawa, T. Waki, M. Horvatić, and C. Berthier, Novel ordered phases in the orthogonal dimer spin system $SrCu_2(BO_3)_2$, Journal of the Physical Society of Japan **79**, 011005 (2010).
[15] H. Kageyama, K. Onizuka, T. Yamauchi, Y. Ueda, S. Hane, H. Mitamura, T. Goto, K. Yoshimura, and K. Kosuge, Anomalous magnetizations in single crystalline $SrCu_2(BO_3)_2$, Journal of the Physical Society of Japan **68**, 1821 (1999).
[16] H. Nojiri, H. Kageyama, K. Onizuka, Y. Ueda, and M. Motokawa, Direct observation of the multiple spin gap excitations in two-dimensional dimer system $SrCu_2(BO_3)_2$, Journal of the Physical Society of Japan **68**, 2906 (1999).
[17] H. Kageyama, M. Nishi, N. Aso, K. Onizuka, T. Yosihama, K. Nukui, K. Kodama, K. Kakurai, and Y. Ueda, Direct evidence for the localized single-triplet excitations and the dispersive multitriplet excitations in $SrCu_2(BO_3)_2$, Phys. Rev. Lett. **84**, 5876 (2000).
[18] H. Kageyama, K. Onizuka, Y. Ueda, M. Nohara, H. Suzuki, and H. Takagi, Low-temperature specific heat study of $SrCu_2(BO_3)_2$ with an exactly solvable ground state, Journal of Experimental and Theoretical Physics **90**, 129 (2000).
[19] P. Lemmens, M. Grove, M. Fischer, G. Güntherodt, V. N. Kotov, H. Kageyama, K. Onizuka, and Y. Ueda, Collective singlet excitations and evolution of raman spectral weights in the 2d spin dimer compound $SrCu_2(BO_3)_2$, Phys. Rev. Lett. **85**, 2605 (2000).
[20] H. Nojiri, H. Kageyama, Y. Ueda, and M. Motokawa, Esr study on the excited state energy spectrum of $SrCu_2(BO_3)_2$ -a central role of multiple-triplet bound states-, Journal of the Physical Society of Japan **72**, 3243 (2003).
[21] B. D. Gaulin, S. H. Lee, S. Haravifard, J. P. Castellan, A. J. Berlinsky, H. A. Dabkowska, Y. Qiu, and J. R. D. Copley, High-resolution study of spin excitations in the singlet ground state of $srcu_2(bo_3)_2$, Phys. Rev. Lett. **93**, 267202 (2004).
[22] A. Zorko, D. Arčon, H. van Tol, L. C. Brunel, and H. Kageyama, X-band esr determination of dzyaloshinsky-moriya interaction in the two-dimensional $SrCu_2(BO_3)_2$ system, Phys. Rev. B **69**, 174420 (2004).
[23] K. Kakurai, K. Nukui, N. Aso, M. Nishi, H. Kadowaki, H. Kageyama, Y. Ueda, L.-P. Regnault, and O. Cépas, Neutron scattering investigation on quantum spin system $SrCu_2(BO_3)_2$, Progress of Theoretical Physics Supplement **159**, 22 (2005).
[24] H. Tsujii, C. R. Rotundu, B. Andraka, Y. Takano, H. Kageyama, and Y. Ueda, Specific heat of the s=1/2 two-dimensional shastry-sutherland antiferromagnet $SrCu_2(BO_3)_2$ in high magnetic fields, Journal of the Physical Society of Japan **80**, 043707 (2011).
[25] S. Bettler, L. Stoppel, Z. Yan, S. Gvasaliya, and A. Zheludev, Sign switching of dimer correlations in $SrCu_2(BO_3)_2$ under hydrostatic pressure, Phys. Rev. Res. **2**, 012010 (2020).
[26] S. Imajo, N. Matsuyama, T. Nomura, T. Kihara, S. Nakamura, C. Marcenat, T. Klein, G. Seyfarth, C. Zhong, H. Kageyama, K. Kindo, T. Momoi, and Y. Kohama, Magnetically hidden state on the ground floor of the magnetic devil's staircase, Phys. Rev. Lett. **129**, 147201 (2022).
[27] A. Koga and N. Kawakami, Quantum phase transitions in the shastry-sutherland model for $SrCu_2(BO_3)_2$, Phys. Rev. Lett. **84**, 4461 (2000).
[28] Y. Takushima, A. Koga, and N. Kawakami, Competing spin-gap phases in a frustrated quantum spin system in two dimensions, Journal of the Physical Society of Japan **70**, 1369 (2001).
[29] A. Läuchli, S. Wessel, and M. Sigrist, Phase diagram of the quadrumerized shastry-sutherland model, Phys. Rev. B **66**, 014401 (2002).
[30] P. Corboz and F. Mila, Tensor network study of the shastry-sutherland model in zero magnetic field, Phys. Rev. B **87**, 115144 (2013).
[31] N. Xi, H. Chen, Z. Y. Xie, and R. Yu, Plaquette valence bond solid to antiferromagnet transition and deconfined quantum critical point of the shastry-sutherland model, Phys. Rev. B **107**, L220408 (2023).
[32] S. Miyahara and K. Ueda, Exact dimer ground state of the two dimensional heisenberg spin system $SrCu_2(BO_3)_2$, Phys. Rev. Lett. **82**, 3701 (1999).
[33] T. Sakurai, M. Tomoo, S. Okubo, H. Ohta, K. Kudo, and Y. Koike, High-field and high-pressure esr measurements of $SrCu_2(BO_3)_2$, Journal of Physics: Conference Series **150**, 042171 (2009).
[34] T. Waki, K. Arai, M. Takigawa, Y. Saiga, Y. Uwatoko, H. Kageyama, and Y. Ueda, A novel ordered phase in $SrCu_2(BO_3)_2$ under high pressure, Journal of the Physical Society of Japan **76**, 073710 (2007).
[35] S. Haravifard, A. Banerjee, J. C. Lang, G. Srajer, D. M. Silevitch, B. D. Gaulin, H. A. Dabkowska, and

T. F. Rosenbaum, Continuous and discontinuous quantum phase transitions in a model two-dimensional magnet, Proceedings of the National Academy of Sciences **109**, 2286 (2012).

[36] T. Sakurai, Y. Hirao, K. Hijii, S. Okubo, H. Ohta, Y. Uwatoko, K. Kudo, and Y. Koike, Direct observation of the quantum phase transition of $SrCu_2(BO_3)_2$ by high-pressure and terahertz electron spin resonance, Journal of the Physical Society of Japan **87**, 033701 (2018).

[37] M. E. Zayed, C. Rüegg, J. Larrea J., A. M. Läuchli, C. Panagopoulos, S. S. Saxena, M. Ellerby, D. F. McMorrow, T. Strässle, S. Klotz, G. Hamel, R. A. Sadykov, V. Pomjakushin, M. Boehm, M. Jiménez-Ruiz, A. Schneidewind, E. Pomjakushina, M. Stingaciu, K. Conder, and H. M. Rønnow, 4-spin plaquette singlet state in the shastry–sutherland compound $SrCu_2(BO_3)_2$, Nature Physics **13**, 962 (2017).

[38] J. Guo, G. Sun, B. Zhao, L. Wang, W. Hong, V. A. Sidorov, N. Ma, Q. Wu, S. Li, Z. Y. Meng, A. W. Sandvik, and L. Sun, Quantum phases of $SrCu_2(BO_3)_2$ from high-pressure thermodynamics, Phys. Rev. Lett. **124**, 206602 (2020).

[39] Y. Cui, L. Liu, H. Lin, K.-H. Wu, W. Hong, X. Liu, C. Li, Z. Hu, N. Xi, S. Li, R. Yu, A. W. Sandvik, and W. Yu, Proximate deconfined quantum critical point in $SrCu_2(BO_3)_2$, Science **380**, 1179 (2023).

[40] K. Onizuka, H. Kageyama, Y. Narumi, K. Kindo, Y. Ueda, and T. Goto, 1/3 magnetization plateau in $SrCu_2(BO_3)_2$ - stripe order of excited triplets -, Journal of the Physical Society of Japan **69**, 1016 (2000).

[41] K. Kodama, M. Takigawa, M. Horvatic, C. Berthier, H. Kageyama, Y. Ueda, S. Miyahara, F. Becca, and F. Mila, Magnetic superstructure in the two-dimensional quantum antiferromagnet $SrCu_2(BO_3)_2$, Science **298**, 395 (2002).

[42] T. Momoi and K. Totsuka, Magnetization plateaus as insulator-superfluid transitions in quantum spin systems, Phys. Rev. B **61**, 3231 (2000).

[43] S. Miyahara and K. Ueda, Superstructures at magnetization plateaus in $SrCu_2(BO_3)_2$, Phys. Rev. B **61**, 3417 (2000).

[44] T. Momoi and K. Totsuka, Magnetization plateaus of the shastry-sutherland model for $SrCu_2(BO_3)_2$ spin-density wave, supersolid, and bound states, Phys. Rev. B **62**, 15067 (2000).

[45] M. Takigawa, K. Kodama, M. Horvatić, C. Berthier, H. Kageyama, Y. Ueda, S. Miyahara, F. Becca, and F. Mila, The 18-magnetization plateau state in the 2d quantum antiferromagnet $SrCu_2(BO_3)_2$: spin superstructure, phase transition, and spin dynamics studied by high-field nmr, Physica B: Condensed Matter **346-347**, 27 (2004), proceedings of the 7th International Symposium on Research in High Magnetic Fields.

[46] K. Kodama, S. Miyahara, M. Takigawa, M. Horvatić, C. Berthier, F. Mila, H. Kageyama, and Y. Ueda, Field-induced effects of anisotropic magnetic interactions in $SrCu_2(BO_3)_2$, Journal of Physics: Condensed Matter **17**, L61 (2005).

[47] S. E. Sebastian, N. Harrison, P. Sengupta, C. D. Batista, S. Francoual, E. Palm, T. Murphy, N. Marcano, H. A. Dabkowska, and B. D. Gaulin, Fractalization drives crystalline states in a frustrated spin system, Proceedings of the National Academy of Sciences **105**, 20157 (2008).

[48] M. Jaime, R. Daou, S. A. Crooker, F. Weickert, A. Uchida, A. E. Feiguin, C. D. Batista, H. A. Dabkowska, and B. D. Gaulin, Magnetostriction and magnetic texture to 100.75 tesla in frustrated $SrCu_2(BO_3)_2$, Proceedings of the National Academy of Sciences **109**, 12404 (2012).

[49] M. Takigawa, M. Horvatić, T. Waki, S. Krämer, C. Berthier, F. Lévy-Bertrand, I. Sheikin, H. Kageyama, Y. Ueda, and F. Mila, Incomplete devil's staircase in the magnetization curve of $SrCu_2(BO_3)_2$, Phys. Rev. Lett. **110**, 067210 (2013).

[50] Y. H. Matsuda, N. Abe, S. Takeyama, H. Kageyama, P. Corboz, A. Honecker, S. R. Manmana, G. R. Foltin, K. P. Schmidt, and F. Mila, Magnetization of $SrCu_2(BO_3)_2$ in ultrahigh magnetic fields up to 118 t, Phys. Rev. Lett. **111**, 137204 (2013).

[51] S. Haravifard, D. Graf, A. E. Feiguin, C. D. Batista, J. C. Lang, D. M. Silevitch, G. Srajer, B. D. Gaulin, H. A. Dabkowska, and T. F. Rosenbaum, Crystallization of spin superlattices with pressure and field in the layered magnet $SrCu_2(BO_3)_2$, Nature Communications **7**, 11956 (2016).

[52] T. Nomura, P. Corboz, A. Miyata, S. Zherlitsyn, Y. Ishii, Y. Kohama, Y. H. Matsuda, A. Ikeda, C. Zhong, H. Kageyama, and F. Mila, Unveiling new quantum phases in the shastry-sutherland compound $SrCu_2(BO_3)_2$ up to the saturation magnetic field, Nature Communications **14**, 3769 (2023).

[53] H. Hirori, A. Doi, F. Blanchard, and K. Tanaka, Single-cycle terahertz pulses with amplitudes exceeding 1 mv/cm generated by optical rectification in linbo3, Applied Physics Letters **98**, 091106 (2011).

[54] M. Sato, T. Higuchi, N. Kanda, K. Konishi, K. Yoshioka, T. Suzuki, K. Misawa, and M. Kuwata-Gonokami, Terahertz polarization pulse shaping with arbitrary field control, Nature Photonics **7**, 724 (2013).

[55] H. A. Hafez, X. Chai, A. Ibrahim, S. Mondal, D. Férachou, X. Ropagnol, and T. Ozaki, Intense terahertz radiation and their applications, Journal of Optics **18**, 093004 (2016).

[56] S. S. Dhillon, M. S. Vitiello, E. H. Linfield, A. G. Davies, M. C. Hoffmann, J. Booske, C. Paoloni, M. Gensch, P. Weightman, G. P. Williams, E. Castro-Camus, D. R. S. Cumming, F. Simoens, I. Escorcia-Carranza, J. Grant, S. Lucyszyn, M. Kuwata-Gonokami, K. Konishi, M. Koch, C. A. Schmuttenmaer, T. L. Cocker, R. Huber, A. G. Markelz, Z. D. Taylor, V. P. Wallace, J. A. Zeitler, J. Sibik, T. M. Korter, B. Ellison, S. Rea, P. Goldsmith, K. B. Cooper, R. Appleby, D. Pardo, P. G. Huggard, V. Krozer, H. Shams, M. Fice, C. Renaud, A. Seeds, A. Stöhr, M. Naftaly, N. Ridler, R. Clarke, J. E. Cunningham, and M. B. Johnston, The 2017 terahertz science and technology roadmap, Journal of Physics D: Applied Physics **50**, 043001 (2017).

[57] B. Liu, H. Bromberger, A. Cartella, T. Gebert, M. Först, and A. Cavalleri, Generation of narrowband, high-intensity, carrier-envelope phase-stable pulses tunable between 4 and 18 thz, Opt. Lett. **42**, 129 (2017).

[58] Y. Mukai, H. Hirori, T. Yamamoto, H. Kageyama, and K. Tanaka, Nonlinear magnetization dynamics of antiferromagnetic spin resonance induced by intense terahertz magnetic field, New Journal of Physics **18**, 013045

(2016).
[59] S. Kovalev, Z. Wang, J.-C. Deinert, N. Awari, M. Chen, B. Green, S. Germanskiy, T. V. A. G. de Oliveira, J. S. Lee, A. Deac, D. Turchinovich, N. Stojanovic, S. Eisebitt, I. Radu, S. Bonetti, T. Kampfrath, and M. Gensch, Selective thz control of magnetic order: new opportunities from superradiant undulator sources, Journal of Physics D: Applied Physics **51**, 114007 (2018).
[60] E. T. Papaioannou and R. Beigang, Thz spintronic emitters: a review on achievements and future challenges, Nanophotonics **10**, 1243 (2021).
[61] A. Leitenstorfer, A. S. Moskalenko, T. Kampfrath, J. Kono, E. Castro-Camus, K. Peng, N. Qureshi, D. Turchinovich, K. Tanaka, A. G. Markelz, M. Havenith, C. Hough, H. J. Joyce, W. J. Padilla, B. Zhou, K.-Y. Kim, X.-C. Zhang, P. U. Jepsen, S. Dhillon, M. Vitiello, E. Linfield, A. G. Davies, M. C. Hoffmann, R. Lewis, M. Tonouchi, P. Klarskov, T. S. Seifert, Y. A. Gerasimenko, D. Mihailovic, R. Huber, J. L. Boland, O. Mitrofanov, P. Dean, B. N. Ellison, P. G. Huggard, S. P. Rea, C. Walker, D. T. Leisawitz, J. R. Gao, C. Li, Q. Chen, G. Valušis, V. P. Wallace, E. Pickwell-MacPherson, X. Shang, J. Hesler, N. Ridler, C. C. Renaud, I. Kallfass, T. Nagatsuma, J. A. Zeitler, D. Arnone, M. B. Johnston, and J. Cunningham, The 2023 terahertz science and technology roadmap, Journal of Physics D: Applied Physics **56**, 223001 (2023).
[62] D. Nicoletti and A. Cavalleri, Nonlinear light–matter interaction at terahertz frequencies, Adv. Opt. Photon. **8**, 401 (2016).
[63] T. Kampfrath, A. Sell, G. Klatt, A. Pashkin, S. Mährlein, T. Dekorsy, M. Wolf, M. Fiebig, A. Leitenstorfer, and R. Huber, Coherent terahertz control of antiferromagnetic spin waves, Nature Photonics **5**, 31 (2011).
[64] T. Kampfrath, K. Tanaka, and K. A. Nelson, Resonant and nonresonant control over matter and light by intense terahertz transients, Nature Photonics **7**, 680 (2013).
[65] C. Vicario, C. Ruchert, F. Ardana-Lamas, P. M. Derlet, B. Tudu, J. Luning, and C. P. Hauri, Off-resonant magnetization dynamics phase-locked to an intense phase-stable terahertz transient, Nature Photonics **7**, 720 (2013).
[66] S. Baierl, J. H. Mentink, M. Hohenleutner, L. Braun, T.-M. Do, C. Lange, A. Sell, M. Fiebig, G. Woltersdorf, T. Kampfrath, and R. Huber, Terahertz-driven nonlinear spin response of antiferromagnetic nickel oxide, Phys. Rev. Lett. **117**, 197201 (2016).
[67] J. Lu, X. Li, H. Y. Hwang, B. K. Ofori-Okai, T. Kurihara, T. Suemoto, and K. A. Nelson, Coherent two-dimensional terahertz magnetic resonance spectroscopy of collective spin waves, Phys. Rev. Lett. **118**, 207204 (2017).
[68] D. Bossini, S. Dal Conte, G. Cerullo, O. Gomonay, R. V. Pisarev, M. Borovsak, D. Mihailovic, J. Sinova, J. H. Mentink, T. Rasing, and A. V. Kimel, Laser-driven quantum magnonics and terahertz dynamics of the order parameter in antiferromagnets, Phys. Rev. B **100**, 024428 (2019).
[69] J. Li, C. B. Wilson, R. Cheng, M. Lohmann, M. Kavand, W. Yuan, M. Aldosary, N. Agladze, P. Wei, M. S. Sherwin, and J. Shi, Spin current from sub-terahertz-generated antiferromagnetic magnons, Nature **578**, 70 (2020).
[70] J. Walowski and M. Münzenberg, Perspective: Ultrafast magnetism and THz spintronics, Journal of Applied Physics **120**, 140901 (2016).
[71] P. Salén, M. Basini, S. Bonetti, J. Hebling, M. Krasilnikov, A. Y. Nikitin, G. Shamuilov, Z. Tibai, V. Zhaunerchyk, and V. Goryashko, Matter manipulation with extreme terahertz light: Progress in the enabling thz technology, Physics Reports **836-837**, 1 (2019).
[72] A. R. Safin, S. A. Nikitov, A. I. Kirilyuk, D. V. Kalyabin, A. V. Sadovnikov, P. A. Stremoukhov, M. V. Logunov, and P. A. Popov, Excitation of terahertz magnons in antiferromagnetic nanostructures: Theory and experiment, Journal of Experimental and Theoretical Physics **131**, 71 (2020).
[73] A. Pimenov, A. A. Mukhin, V. Y. Ivanov, V. D. Travkin, A. M. Balbashov, and A. Loidl, Possible evidence for electromagnons in multiferroic manganites, Nature Physics **2**, 97 (2006).
[74] Y. Takahashi, R. Shimano, Y. Kaneko, H. Murakawa, and Y. Tokura, Magnetoelectric resonance with electromagnons in a perovskite helimagnet, Nature Physics **8**, 121 (2012).
[75] T. Kubacka, J. A. Johnson, M. C. Hoffmann, C. Vicario, S. D. Jong, P. Beaud, S. Grübel, S.-W. Huang, L. Huber, L. Patthey, Y.-D. Chuang, J. J. Turner, G. L. Dakovski, W.-S. Lee, M. P. Minitti, W. Schlotter, R. G. Moore, C. P. Hauri, S. M. Koohpayeh, V. Scagnoli, G. Ingold, S. L. Johnson, and U. Staub, Large-amplitude spin dynamics driven by a thz pulse in resonance with an electromagnon, Science **343**, 1333 (2014).
[76] Z. Wang, J. Wu, W. Yang, A. K. Bera, D. Kamenskyi, A. T. M. N. Islam, S. Xu, J. M. Law, B. Lake, C. Wu, and A. Loidl, Experimental observation of bethe strings, Nature **554**, 219 (2018).
[77] Z. Zhang, F. Sekiguchi, T. Moriyama, S. C. Furuya, M. Sato, T. Satoh, Y. Mukai, K. Tanaka, T. Yamamoto, H. Kageyama, Y. Kanemitsu, and H. Hirori, Generation of third-harmonic spin oscillation from strong spin precession induced by terahertz magnetic near fields, Nature Communications **14**, 1795 (2023).
[78] M. Mochizuki and N. Nagaosa, Theoretically predicted picosecond optical switching of spin chirality in multiferroics, Phys. Rev. Lett. **105**, 147202 (2010).
[79] T. N. Ikeda and M. Sato, High-harmonic generation by electric polarization, spin current, and magnetization, Phys. Rev. B **100**, 214424 (2019).
[80] N. M. Allafi, M. H. Kolodrubetz, M. Bukov, V. Oganesyan, and M. Yarmohammadi, Spin high harmonic generation through terahertz laser-driven phonons, Phys. Rev. B **110**, 064420 (2024).
[81] M. Sato and Y. Morisaku, Two-photon driven magnon-pair resonance as a signature of spin-nematic order, Phys. Rev. B **102**, 060401 (2020).
[82] M. Kanega, T. N. Ikeda, and M. Sato, Linear and nonlinear optical responses in kitaev spin liquids, Phys. Rev. Res. **3**, L032024 (2021).
[83] M. Sato, Y. Sasaki, and T. Oka, Floquet majorana edge mode and non-abelian anyons in a driven kitaev model (2014), arXiv:1404.2010 [cond-mat.str-el].

[84] M. Sato, S. Takayoshi, and T. Oka, Laser-driven multiferroics and ultrafast spin current generation, Phys. Rev. Lett. **117**, 147202 (2016).

[85] S. Higashikawa, H. Fujita, and M. Sato, Floquet engineering of classical systems (2018), arXiv:1810.01103 [cond-mat.str-el].

[86] T. Hirosawa, J. Klinovaja, D. Loss, and S. A. Díaz, Laser-controlled real- and reciprocal-space topology in multiferroic insulators, Phys. Rev. Lett. **128**, 037201 (2022).

[87] R. Yambe and S. Hayami, Symmetry analysis of light-induced magnetic interactions via floquet engineering, Phys. Rev. B **108**, 064420 (2023).

[88] R. Yambe and S. Hayami, Scalar spin chirality induced by a circularly polarized electric field in a classical kagome magnet, Phys. Rev. B **109**, 064428 (2024).

[89] D. Shin, H. Hübener, U. De Giovannini, H. Jin, A. Rubio, and N. Park, Phonon-driven spin-floquet magneto-valleytronics in mos2, Nature Communications **9**, 638 (2018).

[90] A. Gozar, B. S. Dennis, H. Kageyama, and G. Blumberg, Symmetry and light coupling to phononic and collective magnetic excitations in $SrCu_2(BO_3)_2$, Phys. Rev. B **72**, 064405 (2005).

[91] P. A. McClarty, F. Krüger, T. Guidi, S. F. Parker, K. Refson, A. W. Parker, D. Prabhakaran, and R. Coldea, Topological triplon modes and bound states in a shastry–sutherland magnet, Nature Physics **13**, 736 (2017).

[92] D. Wulferding, Y. Choi, S. Lee, M. A. Prosnikov, Y. Gallais, P. Lemmens, C. Zhong, H. Kageyama, and K.-Y. Choi, Thermally populated versus field-induced triplon bound states in the shastry-sutherland lattice $SrCu_2(BO_3)_2$, npj Quantum Materials **6**, 102 (2021).

[93] E. Fogh, M. Nayak, O. Prokhnenko, M. Bartkowiak, K. Munakata, J.-R. Soh, A. A. Turrini, M. E. Zayed, E. Pomjakushina, H. Kageyama, H. Nojiri, K. Kakurai, B. Normand, F. Mila, and H. M. Rønnow, Field-induced bound-state condensation and spin-nematic phase in srcu2(bo3)2 revealed by neutron scattering up to 25.9 t, Nature Communications **15**, 442 (2024).

[94] O. E. Alon, V. Averbukh, and N. Moiseyev, Selection rules for the high harmonic generation spectra, Phys. Rev. Lett. **80**, 3743 (1998).

[95] O. Neufeld, D. Podolsky, and O. Cohen, Floquet group theory and its application to selection rules in harmonic generation, Nature Communications **10**, 405 (2019).

[96] T. N. Ikeda, High-order nonlinear optical response of a twisted bilayer graphene, Phys. Rev. Res. **2**, 032015 (2020).

[97] M. Kanega and M. Sato, High-harmonic generation in graphene under the application of a dc electric current: From perturbative to nonperturbative regime, Phys. Rev. B **110**, 035303 (2024).

[98] O. Neufeld, N. Tancogne-Dejean, U. De Giovannini, H. Hübener, and A. Rubio, Attosecond magnetization dynamics in non-magnetic materials driven by intense femtosecond lasers, npj Computational Materials **9**, 39 (2023).

[99] I. Dzyaloshinsky, A thermodynamic theory of "weak" ferromagnetism of antiferromagnetics, Journal of Physics and Chemistry of Solids **4**, 241 (1958).

[100] T. Moriya, Anisotropic superexchange interaction and weak ferromagnetism, Phys. Rev. **120**, 91 (1960).

[101] S. Miyahara, F. Mila, K. Kodama, M. Takigawa, M. Horvatic, C. Berthier, H. Kageyama, and Y. Ueda, The effects of intra-dimer dzyaloshinsky-moriya interaction on the properties of $SrCu_2(BO_3)_2$ in an external magnetic field, Journal of Physics: Condensed Matter **16**, S911 (2004).

[102] S. Miyahara and F. Mila, The effects of dzyaloshinsky-moriya interaction in the orthogonal dimer heisenberg model for $SrCu_2(BO_3)_2$, Progress of Theoretical Physics Supplement **159**, 33 (2005).

[103] Y. F. Cheng, O. Cépas, P. W. Leung, and T. Ziman, Magnon dispersion and anisotropies in $Srcu_2(BO_3)_2$, Phys. Rev. B **75**, 144422 (2007).

[104] V. V. Mazurenko, S. L. Skornyakov, V. I. Anisimov, and F. Mila, First-principles investigation of symmetric and antisymmetric exchange interactions of $Srcu_2(BO_3)_2$, Phys. Rev. B **78**, 195110 (2008).

[105] T. Chen, C. Guo, P. Sengupta, and D. Poletti, Effects of staggered dzyaloshinskii-moriya interactions in a quasi-two-dimensional shastry-sutherland model, Phys. Rev. B **101**, 064417 (2020).

[106] T. Rõõm, D. Hüvonen, U. Nagel, J. Hwang, T. Timusk, and H. Kageyama, Far-infrared spectroscopy of spin excitations and dzyaloshinskii-moriya interactions in the shastry-sutherland compound $Srcu_2(BO_3)_2$, Phys. Rev. B **70**, 144417 (2004).

[107] K. Sparta, G. J. Redhammer, P. Roussel, G. Heger, G. Roth, P. Lemmens, A. Ionescu, M. Grove, G. Güntherodt, F. Hüning, H. Lueken, H. Kageyama, K. Onizuka, and Y. Ueda, Structural phase transition in the 2d spin dimer compound $SrCu_2(BO_3)_2$, The European Physical Journal B - Condensed Matter and Complex Systems **19**, 507 (2001).

[108] T. Kimura, T. Goto, H. Shintani, K. Ishizaka, T. Arima, and Y. Tokura, Magnetic control of ferroelectric polarization, Nature **426**, 55 (2003).

[109] H. Katsura, N. Nagaosa, and A. V. Balatsky, Spin current and magnetoelectric effect in noncollinear magnets, Phys. Rev. Lett. **95**, 057205 (2005).

[110] M. Mostovoy, Ferroelectricity in spiral magnets, Phys. Rev. Lett. **96**, 067601 (2006).

[111] S.-W. Cheong and M. Mostovoy, Multiferroics: a magnetic twist for ferroelectricity, Nature Materials **6**, 13 (2007).

[112] Y. Tokura, S. Seki, and N. Nagaosa, Multiferroics of spin origin, Reports on Progress in Physics **77**, 076501 (2014).

[113] S. Baierl, M. Hohenleutner, T. Kampfrath, A. K. Zvezdin, A. V. Kimel, R. Huber, and R. V. Mikhaylovskiy, Nonlinear spin control by terahertz-driven anisotropy fields, Nature Photonics **10**, 715 (2016).

[114] T.-h. Arima, Spin-driven ferroelectricity and magneto-electric effects in frustrated magnetic systems, Journal of the Physical Society of Japan **80**, 052001 (2011).

[115] S. Miyahara, Theory of absorption in a frustrated spin gap system $srcu_2(bo_3)_2$ (2023), arXiv:2304.10823 [cond-mat.str-el].

[116] O. Cépas and T. Ziman, Theory of phonon-assisted forbidden optical transitions in spin-gap systems, Phys. Rev. B **70**, 024404 (2004).

[117] S. Kimura, M. Matsumoto, M. Akaki, M. Hagiwara, K. Kindo, and H. Tanaka, Electric dipole spin resonance in a quantum spin dimer system driven by magnetoelec-

tric coupling, Phys. Rev. B **97**, 140406 (2018).
[118] D. Hüvonen, U. Nagel, T. Rõ om, Y. J. Choi, C. L. Zhang, S. Park, and S.-W. Cheong, Magnetic excitations and optical transitions in the multiferroic spin-$\frac{1}{2}$ system $licu_2o_2$, Phys. Rev. B **80**, 100402 (2009).
[119] S. Furukawa, M. Sato, and S. Onoda, Chiral order and electromagnetic dynamics in one-dimensional multiferroic cuprates, Phys. Rev. Lett. **105**, 257205 (2010).
[120] F. Giorgianni, B. Wehinger, S. Allenspach, N. Colonna, C. Vicario, P. Puphal, E. Pomjakushina, B. Normand, and C. Rüegg, Ultrafast frustration breaking and magnetophononic driving of singlet excitations in a quantum magnet, Phys. Rev. B **107**, 184440 (2023).
[121] T. J. Park and J. C. Light, Unitary quantum time evolution by iterative lanczos reduction, J. Chem. Phys. **85**, 5870 (1986).
[122] N. Mohankumar and S. M. Auerbach, On time-step bounds in unitary quantum evolution using the lanczos method, Comput. Phys. Commun. **175**, 473 (2006).
[123] Y. Wang, M. Claassen, B. Moritz, and T. P. Devereaux, Producing coherent excitations in pumped mott antiferromagnetic insulators, Phys. Rev. B **96**, 235142 (2017).
[124] S. Furukawa, T. Dodds, and Y. B. Kim, Ferromagnetically coupled dimers on the distorted shastry-sutherland lattice: Application to $(cucl)lanb_2o_7$, Phys. Rev. B **84**, 054432 (2011).
[125] K. Prabhu, Window functions and their applications in signal processing, Taylor & Francis (2014).
[126] P. Podder, T. Z. Khan, M. H. Khan, and M. M. Rahman, Comparative performance analysis of hamming, hanning and blackman window, International Journal of Computer Applications **96**, 1 (2014).
[127] See Supplemental Material for details. The Supplemental Material also contains Refs. [137–147].
[128] P. Jacobs, Group theory with applications in chemical physics, Cambridge University Press (2005).
[129] M. Dresselhaus, G. Dresselhaus, and A. Jorio, Group theory: Application to the physics of condensed matter, Springer Berlin Heidelberg (2007).
[130] A. Fleischer, O. Kfir, T. Diskin, P. Sidorenko, and O. Cohen, Spin angular momentum and tunable polarization in high-harmonic generation, Nature Photonics **8**, 543 (2014).
[131] O. Kfir, P. Grychtol, E. Turgut, R. Knut, D. Zusin, D. Popmintchev, T. Popmintchev, H. Nembach, J. M. Shaw, A. Fleischer, H. Kapteyn, M. Murnane, and O. Cohen, Generation of bright phase-matched circularly-polarized extreme ultraviolet high harmonics, Nature Photonics **9**, 99 (2015).
[132] H. Eichmann, A. Egbert, S. Nolte, C. Momma, B. Wellegehausen, W. Becker, S. Long, and J. K. McIver, Polarization-dependent high-order two-color mixing, Phys. Rev. A **51**, R3414 (1995).
[133] D. Baykusheva, M. S. Ahsan, N. Lin, and H. J. Wörner, Bicircular high-harmonic spectroscopy reveals dynamical symmetries of atoms and molecules, Phys. Rev. Lett. **116**, 123001 (2016).
[134] K. Ogawa, N. Kanda, Y. Murotani, and R. Matsunaga, Programmable generation of counterrotating bicircular light pulses in the multi-terahertz frequency range (2023), arXiv:2312.04768 [physics.optics].
[135] P. Czarnik, M. M. Rams, P. Corboz, and J. Dziarmaga, Tensor network study of the $m = \frac{1}{2}$ magnetization plateau in the shastry-sutherland model at finite temperature, Phys. Rev. B **103**, 075113 (2021).
[136] Z. Wang and C. D. Batista, Dynamics and instabilities of the shastry-sutherland model, Phys. Rev. Lett. **120**, 247201 (2018).
[137] M. E. Zhitomirsky and H. Tsunetsugu, Magnon pairing in quantum spin nematic, Europhysics Letters **92**, 37001 (2010).
[138] T. Sakai, O. Cépas, and T. Ziman, An electron spin resonance selection rule for spin-gapped systems, Journal of the Physical Society of Japan **69**, 3521 (2000).
[139] C. Boos, S. P. G. Crone, I. A. Niesen, P. Corboz, K. P. Schmidt, and F. Mila, Competition between intermediate plaquette phases in $SrCu_2(BO_3)_2$ under pressure, Phys. Rev. B **100**, 140413 (2019).
[140] A. V. Chubukov, Chiral, nematic, and dimer states in quantum spin chains, Phys. Rev. B **44**, 4693 (1991).
[141] T. Hikihara, L. Kecke, T. Momoi, and A. Furusaki, Vector chiral and multipolar orders in the spin-$\frac{1}{2}$ frustrated ferromagnetic chain in magnetic field, Phys. Rev. B **78**, 144404 (2008).
[142] H. T. Ueda and K. Totsuka, Magnon bose-einstein condensation and various phases of three-dimensonal quantum helimagnets under high magnetic field, Phys. Rev. B **80**, 014417 (2009).
[143] J. Sudan, A. Lüscher, and A. M. Läuchli, Emergent multipolar spin correlations in a fluctuating spiral: The frustrated ferromagnetic spin-$\frac{1}{2}$ heisenberg chain in a magnetic field, Phys. Rev. B **80**, 140402 (2009).
[144] D. A. Schneider, K. Coester, F. Mila, and K. P. Schmidt, Pressure dependence of the magnetization plateaus of $SrCu_2(BO_3)_2$, Phys. Rev. B **93**, 241107 (2016).
[145] M. Sato, T. Hikihara, and T. Momoi, Spin-nematic and spin-density-wave orders in spatially anisotropic frustrated magnets in a magnetic field, Phys. Rev. Lett. **110**, 077206 (2013).
[146] C. Shao, H. Lu, X. Zhang, C. Yu, T. Tohyama, and R. Lu, High-harmonic generation approaching the quantum critical point of strongly correlated systems, Phys. Rev. Lett. **128**, 047401 (2022).
[147] N. Shannon, T. Momoi, and P. Sindzingre, Nematic order in square lattice frustrated ferromagnets, Phys. Rev. Lett. **96**, 027213 (2006).